Protein Expression and Purification **17,** 267–272 (1999)
Article ID prep.1999.1144, available online at http://www.idealibrary.com on IDEAL®

Carboxyl-Terminal Domain of Human Apolipoprotein E: Expression, Purification, and Crystallization

Michael Forstner,*[1] Clare Peters-Libeu,†‡ Emeline Contreras-Forrest,† Yvonne Newhouse,† Mark Knapp,* Bernhard Rupp,* and Karl H. Weisgraber†‡§[,2]

**Biology and Biotechnology Research Program, Lawrence Livermore National Laboratory, Livermore, California 94550; †Gladstone Institute of Cardiovascular Disease, P.O. Box 419100, San Francisco, California 94141-9100; and ‡Cardiovascular Research Institute and §Department of Pathology, University of California, San Francisco, California 94143*

Received May 17, 1999, and in revised form July 15, 1999

Thioredoxin fusion expression vectors for two carboxyl-terminal fragments of human apolipoprotein (apo) E (residues 223–272 and 223–299) were generated from an apoE cDNA with the objective of obtaining structural information on this functionally important region of apoE by X-ray crystallography. A thrombin cleavage recognition site was positioned at the fusion junction to release the apoE fragments from the fusion protein. The fusion proteins were expressed in *Escherichia coli,* isolated from cell lysates by nickel-affinity column chromatography, and cleaved with thrombin. After gel filtration and ion exchange chromatography, yields of each fragment were approximately 14 mg/L. Both fragments bind to the phospholipid dimyristoylphosphatidylcholine in a manner similar to that of the 216–299 fragment of apoE isolated from plasma, which represents the major lipid-binding region of the protein. Orthorhombic crystals of the apoE 223–272 fragment that diffracted to 1.8 Å were obtained in a mixture of 0.1 M imidazole (pH 6.0) and 0.4 M NaOAc (pH 7.0–7.5), containing 30% glycerol. The space group is C222 with cell dimensions of a = 35.17 Å, b = 38.95 Å, and c = 133.27 Å.

Human apolipoprotein (apo)[3] E (299 residues, M_r 35,000) is one of the major soluble apolipoproteins found in plasma. Through its interaction with the low-density lipoprotein receptor family, it plays a key role in plasma cholesterol and triglyceride metabolism (1). ApoE has also been implicated in nerve repair and maintenance (2). Several structural isoforms are known and result from allelic polymorphism (3). The three common isoforms, designated apoE2, apoE3, and apoE4, differ in their cysteine–arginine contents at two polymorphic positions in the protein (residues 112 and 158) (4). This structural heterogeneity has a profound impact on the function of the protein: apoE2 and apoE4 are associated with increased plasma cholesterol levels and an increased risk for heart disease (5–7). Moreover, apoE4 is a major risk factor for Alzheimer's disease (8–10) and other forms of neurodegeneration (11–13).

ApoE contains two structural domains, an amino-terminal domain (residues 1–191; M_r 22,000) and a carboxyl-terminal domain (residues 216–299; M_r 10,000) (14,15). The amino-terminal domain contains the region of the protein that binds to the low-density lipoprotein receptor. The structures of the amino-terminal domains of several isoforms have been determined by X-ray crystallography, which showed that all forms share a four-helix bundle folding motif (16). The three-dimensional structure of the carboxyl-terminal domain is not known but is predicted to be highly helical (17,18), which is consistent with circular dichroism measurements (14).

Three functions have been ascribed to the carboxyl-terminal domain of apoE. First, it contains the major lipid-binding elements of the protein (19). The carboxyl-terminal domain is predicted to contain amphipathic α-helices, the major structural motif by which the soluble apolipoproteins bind lipid (18). Second, intact apoE in the lipid-free state exists as a stable tetramer with tetramerization mediated by the carboxyl-terminal domain (14). Third, in apoE4, but not in the other isoforms, the carboxyl- and amino-terminal do-

[1] Current address: Department of Molecular Biology, Box 590, Biomedical Centrum, Uppsala, S-75124, Sweden.
[2] To whom correspondence should be addressed. Fax (415) 285-5632. E-mail: kweisgraber@gladstone.ucsf.edu.
[3] Abbreviations used: apo, apolipoprotein; DMPC, dimyristoylphosphatidylcholine.

1046-5928/99 $30.00

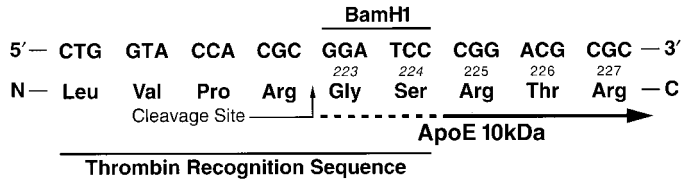

FIG. 1. Thioredoxin apoE carboxyl-terminal fragment expression vector. The nucleotide sequence of the fusion expression vector in the vicinity of the thrombin recognition site at the fusion junction is shown with the corresponding protein sequence below. An apoE cDNA corresponding to residues 223–272 or 223–299 was generated by PCR amplification of an apoE cDNA with primers having *Bam*H1 and *Eco*R1 restriction sites at the 5′ and 3′ ends, respectively. The cDNA was inserted into a *Bam*H1/*Eco*R1-modified pET32NT to generate a thrombin recognition sequence at the fusion junction. The amino-terminal Gly · Ser generated by thrombin cleavage corresponds to residues 223 and 224 in apoE.

mains interact. Mediated by arginine-61 and glutamic acid-255 (20), this domain interaction is thought to be responsible for the unique biochemical and metabolic properties of apoE4 that underlie its detrimental effects in both heart disease and Alzheimer's disease (2).

Since the carboxyl-terminal domain is a functionally important portion of the molecule whose detailed structure is unknown and since our efforts to crystallize the intact protein have been unsuccessful to date, we sought to express functionally relevant fragments of the carboxyl-terminal domain by using recombinant techniques. Here, we describe the production and isolation of two fragments (residues 223–272 and 223–299) and the successful crystallization of both fragments, which yielded diffraction-quality crystals of the 223–272 fragment.

MATERIALS AND METHODS

Vector construction and cloning. The thioredoxin fusion expression vector, pET32NT (Invitrogen) was used to produce the apoE carboxyl-terminal fragments. ApoE cDNAs corresponding to residues 225–272 and 225–299 in apoE were generated by polymerase chain reaction amplification of an apoE-containing vector, pTV194-E3 (21), using primers with *Bam*H1 and *Eco*R1 ends. The cDNAs were inserted into *Bam*H1/*Eco*R1-modified pET32NT. As shown in Fig. 1, a thrombin cleavage recognition site is adjacent to the *Bam*H1 site in the vector. Thrombin cleavage introduces glycine and serine at the amino terminus of the fusion partner, which in the case of apoE coincidentally correspond to positions 223 and 224, respectively.

Protein expression and purification. For protein expression, p10K272 or p10K299 was transformed into *Escherichia coli* strain BL21 (DE3), and transformants expressing high levels of the fusion proteins were grown to mid-log phase in supplemented LB medium at 37°C. Protein expression was induced by adding isopropyl β-thiogalactoside (final concentration, 0.5 mM) to the cells, and the cultures were maintained for 2 h. Cells were harvested by centrifugation at 4000*g*, and the cell pellets were washed twice with ice-cold 0.9% NaCl solution and resuspended in 40 mL of binding buffer (5 mM imidazole, 0.5 mM NaCl, 20 mM Tris–HCl, pH 7.9). Benzonase (2 μL, 25 units/μL; Merck) was added to the suspensions, and the cells were incubated on ice for 5 min and then lysed by ultrasound sonification (Branson medium tip, 3 cycles: 1 min on, 2 min off). Cellular debris was removed by centrifugation at 12,000*g* in an SS-34 rotor (Sorvall, Newtown, CT), and the supernatant was loaded on a nickel-affinity chromatography column, prepared by charging 20 mL of His-tag resin (Novagen) with 50 mM $NiSO_4$ in an Econo-Column (Bio-Rad, Hercules, CA).

The column was washed with 10 column volumes of binding buffer, and the protein was eluted with three column volumes of elution buffer (0.5 M imidazole, 0.5 M NaCl, 20 mM Tris–HCl, pH 7.9). Subsequently, the fusion protein was cleaved by adding thrombin at a ratio of 1:100 (thrombin:uncleaved protein; w/w) for 2 h at room temperature. Thrombin was inactivated by the addition of 2-mercaptoethanol to a final concentration of 1%, and the samples were dialyzed against buffer A (8 M urea, 10 mM Tris–HCl, pH 8.25). Since soluble apolipoproteins tend to self-aggregate, 8 M urea is commonly used in purification steps. Removal of the denaturant results in a fully renatured protein (22). Final purification was performed by high-performance liquid chromatography on a 75 × 7.5-mm DEAE-5PW column (Toso-Haas, Montgomery, PA) employing a linear gradient of 0–0.5 M NaCl in buffer A. The purified 223–272 and 223–299 fragments proteins were dialyzed against 10 mM NH_4HCO_3, pH 7.4.

Protein analysis. Protein purification was monitored by sodium dodecyl sulfate–polyacrylamide gel electrophoresis (SDS–PAGE), and protein concentrations were determined by the Lowry method with bovine serum albumin as the standard (23). The apoE carboxyl-terminal fragments were mixed with dimyristoylphosphatidylcholine (DMPC) at a ratio of 1:3.75 (w/w, protein:DMPC) as previously described (24). The DMPC particles were stained on the surface of carbon fluid grids. Electron micrographs were made at a magnification of 200,000× and imported with a video camera into an Image 1/AT image-analysis system. The particle size was analyzed by automated sizing and counting programs available on system software (mL version 4.03a, Universal Imaging Corp.). Multiple areas on a single grid were sampled.

Crystallization. Initial crystallization trials were performed with Crystal Screen kits (Hampton Research, Laguna Niguel, CA) by using the hanging-drop method. Crystal Screen I condition 25 was modified to

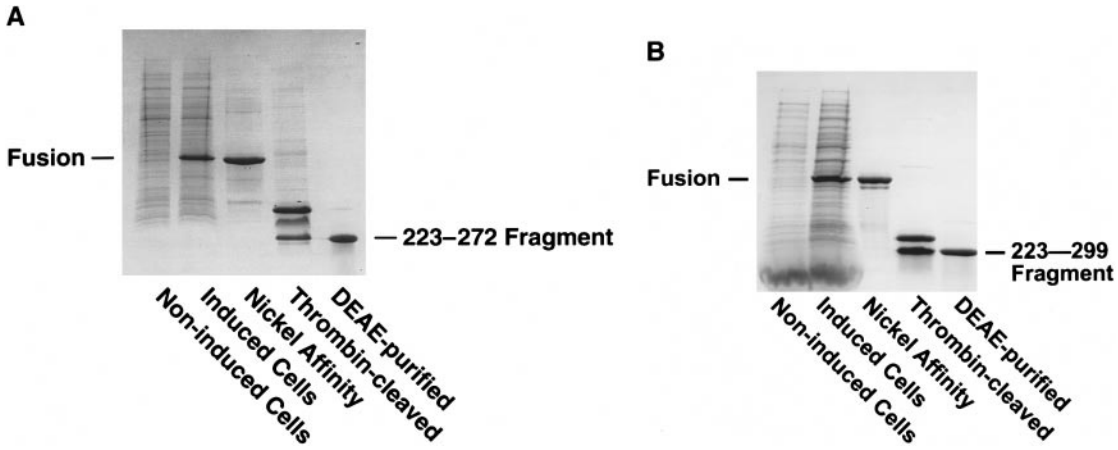

FIG. 2. SDS–PAGE of various stages of purification of the apoE carboxyl-terminal fragments. (A) The 223–272 fragment. (B) The 223–299 fragment.

give optimally sized crystals of the 223–272 fragment. An equal volume of the fragment (5 mg/mL in 10 mM NH_4CO_3) was added to a mixture of 0.1 M imidazole (pH 8.0) and 0.4 M NaOAc (pH 6.8), containing 60% glycerol and equilibrated over a mixture of 0.1 M imidazole (pH 7.0–7.5) and 0.4 M NaOAc (pH 6.8), containing 30% glycerol. Crystals (0.2 × 0.2 × 0.1 mm) grew in 24–48 h and diffracted to 1.8 Å. The 223–299 fragment yielded smaller crystals in solutions of 12% polyethylene glycol 6000, 100 mM NaCl, 100 mM NaOAc (pH 4.6). Conditions have not been further refined.

Crystallographic data collection and analysis. For diffraction studies, crystals were harvested and briefly washed in crystallization buffer, retrieved with a rayon cryoloop, and flash-cooled in liquid nitrogen. Crystals were mounted with cryotongs and kept at near liquid nitrogen temperatures during data collection. Data from native crystals were collected on an ADSCdual multiwire detector system with a rotating Cu-anode X-ray generator (Rigaku, Danvers, MA, RU200, λ = 1.54178 Å) and indexed and integrated with manufacturer-supplied software (see website http://www-structure.llnl.gov for details on instrumentation and cryoprocedures). Synchrotron data were collected under cryoconditions at beamline 5.0.2 with a 2 × 2 module ADSC Quantum 4 CCD detector at the Advanced Light Source (Lawrence Berkeley Laboratory, Berkeley, CA). Data were autoindexed, integrated, and merged with MOSFLM and SCALA of the CCP4 program suite (25). Self-rotation functions were calculated with the program glrf (26) using step sizes of 10° in ϕ, ψ, and κ for the initial search. The positions of peaks corresponding to noncrystallographic symmetry were further refined by using a fine-grid search with step sizes of 1° in the range of ±5° of all the angles of the initial peaks.

RESULTS AND DISCUSSION

Our strategy for obtaining structural information on the carboxyl-terminal domain of apoE was to generate two fragments, spanning residues 223–272 and 223–299, with our thioredoxin fusion expression vector (27) and to crystallize either or both fragments. Previously we used this approach to determine the structure of the amino-terminal fragment of apoE (residues 1–191) (16). In addition, we determined that neither internal deletion of residues 186–222 nor carboxyl-terminal deletion of residues 273–299 had any effect on the protein with respect to lipoprotein binding, indicating that the major lipid-binding elements were contained within residues 223–272 (28). Beginning at position 223 also offered the advantage that, after thrombin digestion, the glycyl and seryl residues contained within the thrombin recognition sequence and added to the amino-terminus of the fusion partner of thioredoxin are identical to the amino acids at positions 223 and 224, respectively, in apoE.

Various stages of the purification procedure, as monitored by SDS–PAGE, are shown in Fig. 2, and the yields are presented in Table 1. Both recombinant proteins were obtained in final yields of approximately 14 mg/L cell culture in the two-step chromatographic procedure. Because the carboxyl-terminal domain of apoE is responsible for lipid binding, we assessed the structural integrity of each recombinant protein by determining its ability to form characteristic discoidal particles when complexed with phospholipid and comparing them with the particles formed by the plasma-derived thrombolytic fragment (residues 216–299) (29). When complexed with DMPC, the 223–299 fragment formed particles similar in size to those found with plasma-derived fragment (15.1 ± 2.9 versus 16.2 ± 2.6 nm, mean ± SD). The 223–272 fragment

TABLE 1

Yield Data for the 223–272 and 223–299 ApoE Fragments

Fragment	Yield (mg/L of culture)			
	Induced cells[a]	Nickel affinity	Thrombin digest	DEAE column
223–272	75 (24)[b]	62 (19.8)[b]	18.2[c]	14.0[d]
223–299	77 (22.3)[b]	71 (20.6)[b]	16.4[c]	13.7[d]

[a] There were approximately 2 g wet wt of cells and approximately 250 mg total protein in the cell lysate supernatant per liter of culture.

[b] Amount of thioredoxin fusion estimated by SDS–PAGE; numbers in parentheses are estimated amounts of the apoE fragment.

[c] Amount of the apoE fragment estimated from Lowry protein analysis of thrombin digest mixture and SDS–PAGE analysis.

[d] Amount of purified fragment based on Lowry protein analysis.

TABLE 2

Data Collection Statistics for p10K272

Space group	C222
a (Å)	35.17
b (Å)	38.95
c (Å)	133.27
d_{min} (Å)[a]	1.8
Observations (n)	71752
Unique reflections (n)	4946
Data completeness	99.2%
R_{merge}[b](%)	10.2
$\langle I/\sigma_{(I)}\rangle$	17.7
Matthews coefficient[c] V_M (Å^3/Da)	1.91
Solvent content[c] (%)	36%
Molecules per asymmetric unit	2

[a] d_{min} = the smallest d spacing for which reflections were measured.

[b] $R_{merge} = \Sigma_i(\Sigma_j | I_{ij} - \langle I_i\rangle|)\Sigma_i\langle I_i\rangle$, where I_{ij}, is the scaled intensity of the jth observation of each unique reflection i and $\langle I_i\rangle$ is the mean value.

[c] Based on the assumption of two molecules in the asymmetric unit.

also formed disks, but they were slightly larger than those formed by the recombinant 223–299 fragment or the plasma-derived fragments (mean 23.5 ± 5.2 nm).

Crystallization attempts yielded crystals of both recombinant proteins; however, only crystals of the 223–272 fragments were of diffraction quality (Fig. 3). The orthorhombic 223–272 crystals diffract to beyond 1.8-Å resolution at near liquid nitrogen temperatures. The space group is C222 (No. 21, z = 8) with unit cell dimensions of a = 35.17 Å, b = 38.95 Å, c = 133.27 Å. The results from initial crystallographic analysis are summarized in Table 2.

Calculation of the Matthews coefficient V_M (30) allows the solvent content of the crystal and the likely

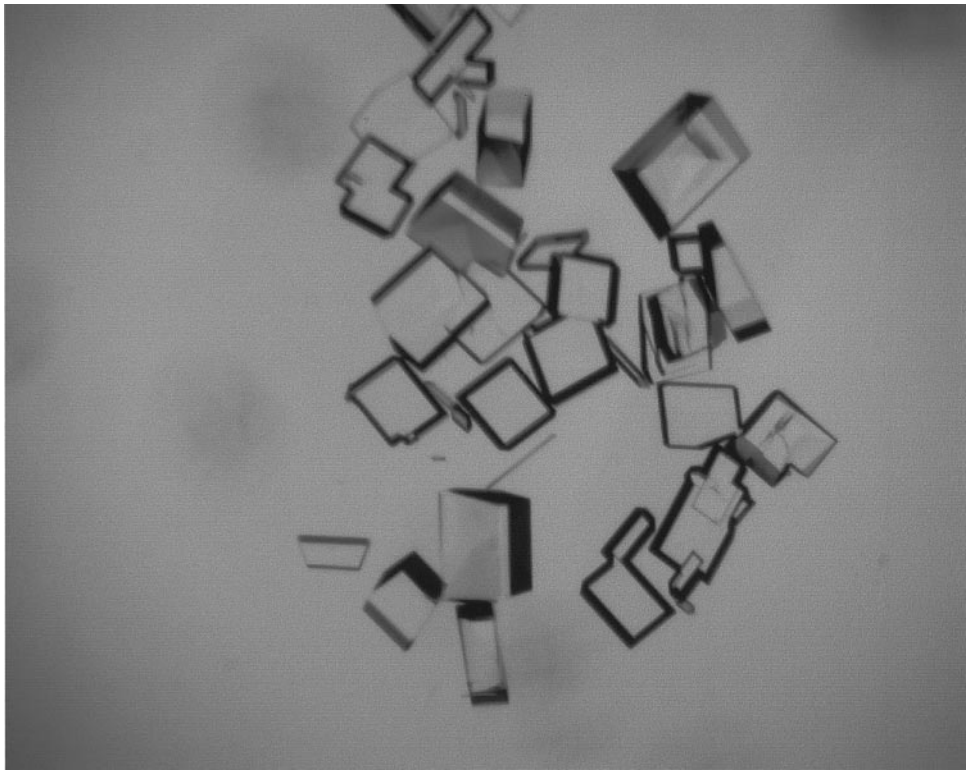

FIG. 3. Crystals of the apoE 223–272 fragment grown by the hanging-drop method.

number of molecules in the asymmetric unit to be estimated. Assuming one molecule of 223–272 fragment per asymmetric unit, we obtained a V_M of 3.82 Å^3/Da, which corresponds to a solvent content of 68%; assuming two molecules per asymmetric unit, we obtained a V_M of 1.91 Å^3/Da, indicating a solvent content of 36%. The lower solvent content obtained with the latter assumption and the more typical value of 1.91 for V_M are consistent with the strong diffraction of the 223–272 fragment crystals (diffraction limit 1.8 Å).

The putative presence of dimers in the asymmetric unit prompted us to search for noncrystallographic symmetry elements. A self-rotation function calculated with the program glrf (26) revealed a weak peak at a κ angle of 19° (plus the corresponding peak at 161° generated by crystallographic twofold symmetry), indicating the presence of a noncrystallographic symmetry operator relating two molecules by a 19° rotation relative to each other. If two α-helices pack at 20° relative to each other, one of the tightest helix–helix packing arrangements possible is found by packing the ridges of one helix into the grooves of the other (31). Such an arrangement could generate a corresponding weak noncrystallographic symmetry axis as revealed in our self-rotation maps.

The carboxyl-terminal domain of apoE is predicted to be highly helical with one long class A amphipathic helix encompassing residues 225–266 (18). Class A amphipathic helices are the major structural motif by which the soluble plasma apolipoproteins interact with lipid (18). The presence of the long class A helix in the carboxyl-terminal region of apoE is consistent with its known lipid-binding properties. Thus, determination of the structure of carboxyl-terminal region of apoE will likely provide important new insights into the structure and function of this critical domain of the protein.

ACKNOWLEDGMENTS

The authors thank David Sanan, Ph.D., and Dale Newland for negative staining electron microscopy, Sharon Israeli for technical assistance, Denise Murray and Kerry Humphrey for manuscript preparation, John C. W. Carroll and Neila Shea for graphics, Chris Goodfellow and Stephen Gonzales for photography, and Stephen Ordway and Gary Howard for editorial assistance. This work was supported by NIH Program Project Grant HL 41633 and by the United States Department of Energy at Lawrence Livermore National Laboratory under Contract W-7405-Eng-48. The work described was carried out in part at the General Clinical Research Center, San Francisco General Hospital Medical Center, with support from a grant from the National Center for Research Resources, NIH. The Macromolecular Crystallography Facility at the Advanced Light Source is principally funded by the Office of Biological and Environmental Research of the Department of Energy with contributions from Lawrence Berkeley National Laboratory, Amgen, Roche Biosciences, University of California at Berkeley, Genetics Institute, and Lawrence Livermore National Laboratory.

REFERENCES

1. Mahley, R. W. (1988) Apolipoprotein E: Cholesterol transport protein with expanding role in cell biology. *Science* **240,** 622–630.
2. Weisgraber, K. H., and Mahley, R. W. (1996) Human apolipoprotein E: The Alzheimer's disease connection. *FASEB J.* **10,** 1485–1494.
3. Zannis, V. I., and Breslow, J. L. (1981) Human very low density lipoprotein apolipoprotein E isoprotein polymorphism is explained by genetic variation and posttranslational modification. *Biochemistry* **20,** 1033–1041.
4. Weisgraber, K. H. (1994) Apolipoprotein E: Structure–function relationships. *Adv. Protein Chem.* **45,** 249–302.
5. Utermann, G., Hardewig, A., and Zimmer, F. (1984) Apolipoprotein E phenotypes in patients with myocardial infarction. *Hum. Genet.* **65,** 237–241.
6. Luc, G., Bard, J.-M., Arveiler, D., Evans, A., Cambou, J.-P., Bingham, A., Amouyel, P., Schaffer, P., Ruidavets, J.-B., Cambien, F., Fruchart, J.-C., and Ducimetiere, P. (1994) Impact of apolipoprotein E polymorphism on lipoproteins and risk of myocardial infarction. The ECTIM study. *Arterioscler. Thromb.* **14,** 1412–1419.
7. Eichner, J. E., Kuller, L. H., Orchard, T. J., Grandits, G. A., McCallum, L. M., Ferrell, R. E., and Neaton, J. D. (1993) Relation of apolipoprotein E phenotype to myocardial infarction and mortality from coronary artery disease. *Am. J. Cardiol.* **71,** 160–165.
8. Strittmatter, W. J., Saunders, A. M., Schmechel, D., Pericak-Vance, M., Enghild, J., Salvesen, G. S., and Roses, A. D. (1993) Apolipoprotein E: High-avidity binding to β-amyloid and increased frequency of type 4 allele in late-onset familial Alzheimer disease. *Proc. Natl. Acad. Sci. USA.* **90,** 1977–1981.
9. Corder, E. H., Saunders, A. M., Strittmatter, W. J., Schmechel, D. E., Gaskell, P. C., Small, G. W., Roses, A. D., Haines, J. L., and Pericak-Vance, M. A. (1993) Gene dose of apolipoprotein E type 4 allele and the risk of Alzheimer's disease in late onset families. *Science* **261,** 921–923.
10. Saunders, A. M., Strittmatter, W. J., Schmechel, D., St George-Hyslop, P. H., Pericak-Vance, M. A., Joo, S. H., Rosi, B. L., Gusella, J. F., Crapper-MacLachlan, D. R., Alberts, M. J., Hulette, C., Crain, B., Goldgaber, D., and Roses, A. D. (1993) Association of apolipoprotein E allele ϵ4 with late-onset familial and sporadic Alzheimer's disease. *Neurology.* **43,** 1467–1472.
11. Mayeux, R., Ottman, R., Maestre, G., Ngai, C., Tang, M.-X., Ginsberg, H., Chun, M., Tycko, B., and Shelanski, M. (1995) Synergistic effects of traumatic head injury and apolipoprotein-ϵ4 in patients with Alzheimer's disease. *Neurology* **45,** 555–557.
12. Slooter, A. J. C., Tang, M.-X., van Duijn, C. M., Stern, Y., Ott, A., Bell, K., Breteler, M. M. B., Van Broeckhoven, C., Tatemichi, T. K., Tycko, B., Hofman, A., and Mayeux, R. (1997) Apolipoprotein E ϵ4 and the risk of dementia with stroke. A population-based investigation. *J. Am. Med. Assoc.* **277,** 818–821.
13. Teasdale, G. M., Nicoll, J. A. R., Murray, G., and Fiddes, M. (1997) Association of apolipoprotein E polymorphism with outcome after head injury. *Lancet* **350,** 1069–1071.
14. Aggerbeck, L. P., Wetterau, J. R., Weisgraber, K. H., Wu, C.-S. C., and Lindgren, F. T. (1988) Human apolipoprotein E3 in aqueous solution. II. Properties of the amino- and carboxyl-terminal domains. *J. Biol. Chem.* **263,** 6249–6258.
15. Wetterau, J. R., Aggerbeck, L. P., Rall, S. C., Jr., and Weisgraber, K. H. (1988) Human apolipoprotein E3 in aqueous solution. I. Evidence for two structural domains. *J. Biol. Chem.* **263,** 6240–6248.
16. Wilson, C., Wardell, M. R., Weisgraber, K. H., Mahley, R. W., and Agard, D. A. (1991) Three-dimensional structure of the LDL

receptor-binding domain of human apolipoprotein E. *Science* **252,** 1817–1822.

17. Rall, S. C., Jr., Weisgraber, K. H., and Mahley, R. W. (1982) Human apolipoprotein E. The complete amino acid sequence. *J. Biol. Chem.* **257,** 4171–4178.
18. Segrest, J. P., Jones, M. K., De Loof, H., Brouillette, C. G., Venkatachalapathi, Y. V., and Anantharamaiah, G. M. (1992) The amphipathic helix in the exchangeable apolipoproteins: A review of secondary structure and function. *J. Lipid Res.* **33,** 141–166.
19. Weisgraber, K. H. (1990) Apolipoprotein E distribution among human plasma lipoproteins: Role of the cysteine–arginine interchange at residue 112. *J. Lipid Res.* **31,** 1503–1511.
20. Dong, L.-M., and Weisgraber, K. H. (1996) Human apolipoprotein E4 domain interaction. Arginine 61 and glutamic acid 255 interact to direct the preference for very low density lipoproteins. *J. Biol. Chem.* **271,** 19053–19057.
21. Vogel, T., Weisgraber, K. H., Zeevi, M. I., Ben-Artzi, H., Levanon, A. Z., Rall, S. C., Jr., Innerarity, T. L., Hui, D. Y., Taylor, J. M., Kanner, D., Yavin, Z., Amit, B., Aviv, H., Gorecki, M., and Mahley, R. W. (1985) Human apolipoprotein E expression in *Escherichia coli:* Structural and functional identity of the bacterially produced protein with plasma apolipoprotein E. *Proc. Natl. Acad. Sci. USA.* **82,** 8696–8700.
22. Rall, S. C., Jr., Weisgraber, K. H., and Mahley, R. W. (1986) Isolation and characterization of apolipoprotein E. *Methods Enzymol.* **128,** 273–287.
23. Lowry, O. H., Rosebrough, N. J., Farr, A. L., and Randall, R. J. (1951) Protein measurement with the Folin phenol reagent. *J. Biol. Chem.* **193,** 265–275.
24. Innerarity, T. L., Pitas, R. E., and Mahley, R. W. (1979) Binding of arginine-rich (E) apoprotein after recombination with phospholipid vesicles to the low density lipoprotein receptors of fibroblasts. *J. Biol. Chem.* **254,** 4186–4190.
25. Collaborative Computational Project Number 4 (1994) The *CCP4* suite: Programs for protein crystallography. *Acta Crystallogr. D* **50,** 760–763.
26. Tong, L. (1993) *REPLACE,* a suite of computer programs for molecular-replacement calculations. *J. Appl. Crystallogr.* **26,** 748–751.
27. Morrow, J. A., Arnold, K. S., and Weisgraber, K. H. (1999) Functional characterization of apolipoprotein E isoforms overexpressed in *Escherichia coli. Protein Expression Purif.* **16,** 224–230.
28. Dong, L.-M., Wilson, C., Wardell, M. R., Simmons, T., Mahley, R. W., Weisgraber, K. H., and Agard, D. A. (1994) Human apolipoprotein E. Role of arginine 61 in mediating the lipoprotein preferences of the E3 and E4 isoforms. *J. Biol. Chem.* **269,** 22358–22365.
29. Innerarity, T. L., Friedlander, E. J., Rall, S. C., Jr., Weisgraber, K. H., and Mahley, R. W. (1983) The receptor-binding domain of human apolipoprotein E. Binding of apolipoprotein E fragments. *J. Biol. Chem.* **258,** 12341–12347.
30. Matthews, B. W. (1968) Solvent content of protein crystals. *J. Mol. Biol.* **33,** 491–497.
31. Chothia, C., Levitt, M., and Richardson, D. (1977) Structure of proteins: Packing of α-helices and pleated sheets. *Proc. Natl. Acad. Sci. USA* **74,** 4130–4134.